

Why Structurally Different Cyclic Peptides Can Be Glycomimetics of the HNK-1 Carbohydrate Antigen

Anirban Bhunia,[†] Subramanian Vivekanandan,[‡] Thomas Eckert,[§] Monika Burg-Roderfeld,[§] Rainer Wechselberger,^{||} Julija Romanuka,^{||} Dirk Bächle,[±] Andrei V. Kornilov,[#] Claus-Wilhelm von der Lieth,^{○,¶} Jesús Jiménez-Barbero,[▽] Nikolay E. Nifantiev,[#] Melitta Schachner,[▲] Norbert Sewald,[±] Thomas Lütteke,[§] and Hans-Christian Siebert^{*,§}

Institut für Biochemie und Endokrinologie, Veterinärmedizinische Fakultät, Justus-Liebig-Universität Giessen, Frankfurter Str. 100, 35392 Giessen, Germany

Received January 13, 2009; Revised Manuscript Received May 28, 2009; E-mail: Hans-Christian.Siebert@vetmed.uni-giessen.de

Abstract: The cyclic peptides c-(LSETTI) and c-(RTL PFS) are of potential clinical interest—they stimulate neurite outgrowth in a way that is similar to the effects of the HNK-1 (human natural killer cell-1) antigenic carbohydrate chains, which are terminated by 3'-sulfated glucuronic acid attached to an *N*-acetylglucosamine unit. To investigate the structure–activity relationships of the ability of the cyclic peptides to mimic HNK-1 carbohydrates, conformational analysis and examination of hydrophobic and hydrophilic patterns were performed and compared with the characteristics of a synthetic HNK-1 trisaccharide derivative. Data obtained demonstrate that both the trisaccharide and the glycomimetic peptide c-(LSETTI) exhibit a similar relationship between their hydrophobic moieties and their negatively charged sites. However, the second cyclic glycomimetic peptide investigated here, c-(RTL PFS), has a positively charged group as a potential contact point due to its Arg residue. Therefore, we studied the amino acid composition of all known receptor structures in the Protein Data Bank that are in contact with uronic acid and/or sulfated glycans. Interactions of the HNK-1 trisaccharide, c-(LSETTI), and c-(RTL PFS) with a laminin fragment involved in HNK-1 carbohydrate binding (i.e., the 21mer peptide: KGVSSRSYVGCINKLEISRST) were also analyzed. Because the structure of the HNK-1-binding laminin domain is not available in the Protein Data Bank, we used the HNK-1-binding 21mer peptide fragment of laminin for the construction of a model receptor that enabled us to compare the molecular interplay of the HNK-1 trisaccharide and the two cyclopeptides c-(LSETTI) and c-(RTL PFS) with a reliable receptor structure in considerable detail.

Introduction

Glycan chains covalently linked to the protein backbone of cell adhesion molecules are increasingly recognized to play important roles in cell–cell recognition and other interaction

processes in the extracellular matrix (for recent reviews, see^{1–4}). Glycomimetics of these glycan chains are of clinical importance and can be considered as a new class of potential therapeutics. Such glycomimetics may have a carbohydrate-based character^{5–9} or they can consist entirely of amino acid residues, as described here. A glycan chain of particular interest is the human natural

[†] Current address: School of Biological Sciences, 60 Nanyang Drive, Nanyang Technological University, Singapore 637551.

[‡] *Structural Biology/NMR Spectroscopy*, U.S. Food & Drug Administration, NIH campus, Bethesda, 20892.

[§] Institut für Biochemie und Endokrinologie, Justus-Liebig-Universität Giessen.

^{||} Utrecht Facility for High-resolution NMR, Bijvoetcenter for Biomolecular Research Utrecht University, Padualaan 8, 3584CH Utrecht, The Netherlands.

[±] Department of Chemistry, Organic and Bioorganic Chemistry, Bielefeld University, Universitätsstrasse 25, 33615 Bielefeld, Germany.

[#] Laboratory of Glycoconjugate Chemistry, N.D. Zelinsky Institute of Organic Chemistry, Russian Academy of Sciences, Leninsky prospect, 47, Moscow B-334, 119991 Russia.

[○] Dr. Claus-Wilhelm von der Lieth passed away on November 16, 2007.

[¶] Zentrale Spektroskopie, Deutsches Krebsforschungszentrum Im Neuenheimer Feld 280, 69120 Heidelberg, Germany.

[▽] Departamento de Estructura y función de proteínas, Centro de Investigaciones Biológicas, CSIC, Ramiro de Maeztu 9, 28040 Madrid, Spain.

[▲] Zentrum für Molekulare Neurobiologie, Universität Hamburg, Martinistrasse 52, 20246 Hamburg, Germany.

- (1) Kleene, R.; Schachner, M. *Nat. Rev. Neurosci.* **2004**, *5*, 195.
- (2) Gabius, H. J.; Siebert, H. C.; André, S.; Jiménez-Barbero, J.; Rüdiger, H. *Chembiochem* **2004**, *5*, 740.
- (3) *The Sugar Code. Fundamentals of Glycoscience*; Gabius, H. J., Ed.; Wiley-VCH: Weinheim, Germany, 2009.
- (4) Solís, D.; Jiménez-Barbero, J.; Kaltner, H.; Romero, A.; Siebert, H. C.; von der Lieth, C. W.; Gabius, H. *J. Cells Tissues Organs* **2001**, *168*, 5.
- (5) Arnusch, C. J.; André, S.; Valentini, P.; Lensch, M.; Russwurm, R.; Siebert, H. C.; Fischer, M. J.; Gabius, H. J.; Pieters, R. *J. Bioorg. Med. Chem. Lett.* **2004**, *14*, 1437.
- (6) Bernardi, A.; Potenza, D.; Capelli, A. M.; Garcia-Herrero, A.; Cañada, F. J.; Jiménez-Barbero, J. *Chemistry* **2002**, *8*, 4597.
- (7) Mikkelsen, L. M.; Hernaiz, M. J.; Martin-Pastor, M.; Skrydstrup, T.; Jiménez-Barbero, J. *J. Am. Chem. Soc.* **2002**, *124*, 14940.
- (8) André, S.; Pei, Z.; Siebert, H. C.; Ramstrom, O.; Gabius, H. J. *Bioorg. Med. Chem.* **2006**, *14*, 6314.
- (9) Fernández-Alonso, M. d. C.; Cañada, F. J.; Solís, D.; Cheng, X.; Kumaran, G.; André, S.; Siebert, H.-C.; Mootoo, D. R.; Gabius, H.-J.; Jiménez-Barbero, J. *Eur. J. Org. Chem.* **2004**, *2004*, 1604.

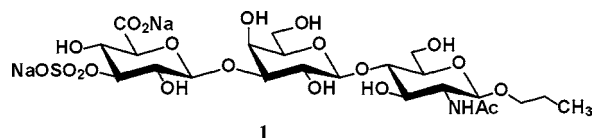


Figure 1. Trisaccharide **1** shows consensus with HNK-1 epitope 3-*O*-sulfo GlcA β (1 \rightarrow 3)Gal β (1 \rightarrow 4)GlcNAc β .

killer cell-1 epitope (HNK-1), which is a characteristic ligand for many neural cell adhesion molecules such as NCAM (neural cell adhesion molecule), the immunoglobulin superfamily molecules L1, F3/contactin, TAG-1, integrins and the extracellular matrix glycoproteins tenascin-R as well as tenascin-C.¹ The HNK-1 trisaccharide sequence with 3'-sulfated glucuronic acid attached to *N*-acetylglucosamine (as in trisaccharide **1** in Figure 1) occurs as the terminal part of a number of glycan chains, thereby acting as a HNK-1 structural determinant.¹⁰

In the peripheral nervous system HNK-1 is found on *N*-glycans of the immunoglobulin superfamily proteins P0 and MAG (myelin-associated glycoprotein), which are involved in the formation and maintenance of myelin.^{11–15} The HNK-1 glycan plays an important role in preferential motor reinnervation. In particular, it is crucial for taking the right path between two nerve branches when severed motor axons in the femoral nerve regenerate into the motor but not into the sensory branch of this nerve.^{16,17} After traumatic lesion of the femoral nerve, HNK-1 acts as an intrinsic molecular effector for Schwann cells associated with motor neurons that have beneficial effects on correct reinnervation after an injury.¹⁸

Peptides that functionally and/or structurally mimic oligosaccharides, such as the cyclic hexapeptides c-(LSETTI) (**2**) and c-(RTLPSF) (**3**) (please see Scheme 1) offer an uncomplicated and promising alternative for interfering with the interactions between complex carbohydrates and their receptors.^{19–23} Cyclic peptides are especially suited because of their high conformational and metabolic stability. The two cyclic hexapeptides display a higher affinity to an HNK-1 receptor than the originally isolated 15mer or 8mer linear peptides mimicking HNK-1.^{23,24} Since the glycomimetic hexapeptides **2** and **3** were shown to

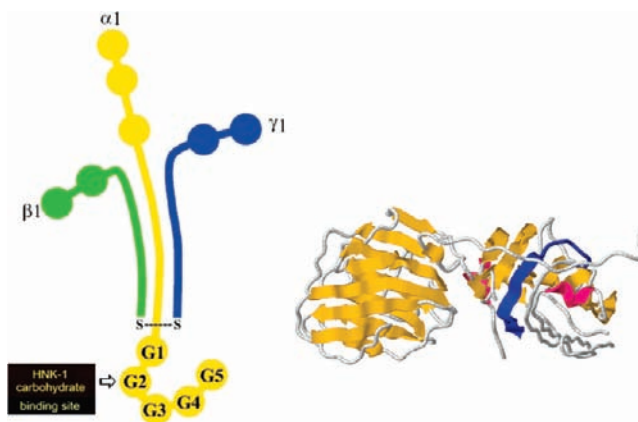


Figure 2. Schematic structure of the distal portion of the long arm of laminin^{26,28} (left). Three-dimensional structure of the G4 and G5 domain of the laminin α subunit (right). The crucial part of the 21mer peptide laminin fragment KGVSSRSYVGCINKLEISRST (**4**) of the G2 domain can also be found in the G5 domain from which the X-ray structure is known. The crucial part is displayed in the G5 domain as blue strand.

specifically enhance neurite outgrowth in a similar way to that of HNK-1,^{16,17} they can be considered as potential therapeutic molecules with clinical relevance.

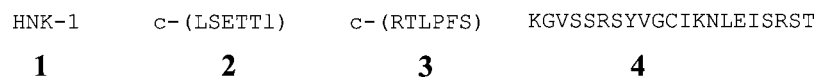
By using a strategic combination of NMR spectroscopic experiments, a database search, and molecular modeling methods (molecular dynamics simulations as well as molecular docking), we learned how the different functional groups of the three ligands under study (the HNK-1 trisaccharide **1** and cyclic peptides **2** and **3**) and the crucial amino acids of a HNK-1 receptor must interact with each other to establish a stable complex. We started with a structural comparison between these three ligands. A molecular modeling-based comparison between the NMR-derived solution structure of the cyclic hexapeptide c-(LSETTI) in water and that of the HNK-1 trisaccharide provides an answer as to why these two differently shaped molecules can interact in a similar way with the HNK-1 binding site of laminin. The other cyclic glycomimetic peptide, c-(RTLPSF), however, has a positively charged group as a potential contact point due to its Arg residue. In this case, a high affinity to a HNK-1 receptor cannot be explained by similarities in charges and polarities between different parts of a glycan and its glycomimetic peptide. Here it is absolutely essential to assemble information about receptor structures interacting with negatively charged carbohydrate moieties of all known protein-carbohydrate complexes in the Protein Data Bank (PDB at www.pdb.org).²⁵ The abundance of the amino acids that interact with uronic acid or sulfated carbohydrates was analyzed with help of a database search (3'-sulfated glucuronic acid is the terminal unit in HNK-1 chains, see Figure 1).

Since there is no structure of an HNK-1 receptor complex available in the database, we focused on laminin in order to construct a reasonable model of an HNK-1 receptor. Laminin consists of a coiled-coil rod contributed by the C-terminal portions of the α 1, β 1 and γ 1 chains. The β 1 and γ 1 chains are connected by a disulfide bond and noncovalently associated with the α 1 chain. The C-terminal end of the α 1 chain is composed of five similar G subdomains. Binding sites for heparin, heparan

- (10) Voshol, H.; van Zuylen, C. W.; Orberger, G.; Vliegthart, J. F. G.; Schachner, M. *J. Biol. Chem.* **1996**, *271*, 22957.
- (11) Kruse, J.; Mailhammer, R.; Wernecke, H.; Faissner, A.; Sommer, I.; Goridis, C.; Schachner, M. *Nature* **1984**, *311*, 153.
- (12) Kruse, J.; Keilhauer, G.; Faissner, A.; Timpl, R.; Schachner, M. *Nature* **1985**, *316*, 146.
- (13) Schneider-Schaulies, J.; Kirchhoff, F.; Archelos, J.; Schachner, M. *Neuron* **1991**, *7*, 995.
- (14) Löw, K.; Orberger, G.; Schmitz, B.; Martini, R.; Schachner, M. *Eur. J. Neurosci.* **1994**, *6*, 1773.
- (15) Schachner, M.; Bartsch, U. *Glia* **2000**, *29*, 154.
- (16) Eberhardt, K. A.; Irintchev, A.; Al-Majed, A. A.; Simova, O.; Brushart, T. M.; Gordon, T.; Schachner, M. *Exp. Neurol.* **2006**, *198*, 500.
- (17) Simova, O.; Irintchev, A.; Mehanna, A.; Liu, J.; Dihne, M.; Bächle, D.; Sewald, N.; Loers, G.; Schachner, M. *Ann. Neurol.* **2006**, *60*, 430.
- (18) Martini, R.; Schachner, M.; Brushart, T. M. *J. Neurosci.* **1994**, *14*, 7180.
- (19) Vyas, N. K.; Vyas, M. N.; Chervenak, M. C.; Bundle, D. R.; Pinto, B. M.; Quijcho, F. A. *Proc. Natl. Acad. Sci. U.S.A.* **2003**, *100*, 15023.
- (20) Johnson, M. A.; Rotondo, A.; Pinto, B. M. *Biochemistry* **2002**, *41*, 2149.
- (21) Johnson, M. A.; Jaseja, M.; Zou, W.; Jennings, H. J.; Copie, V.; Pinto, B. M.; Pincus, S. H. *J. Biol. Chem.* **2003**, *278*, 24740.
- (22) Johnson, M. A.; Eniade, A. A.; Pinto, B. M. *Bioorg. Med. Chem.* **2003**, *11*, 781.
- (23) Bächle, D.; Loers, G.; Guthöhrlein, E. W.; Schachner, M.; Sewald, N. *Angew. Chem., Int. Ed.* **2006**, *45*, 6582.
- (24) Simon-Haldi, M.; Mantel, N.; Franke, J.; Voshol, H.; Schachner, M. *J. Neurochem.* **2002**, *83*, 1380.

- (25) Berman, H. M.; Westbrook, J.; Feng, Z.; Gilliland, G.; Bhat, T. N.; Weissig, H.; Shindyalov, I. N.; Bourne, P. E. *Nucleic Acids Res.* **2000**, *28*, 235.

Scheme 1



sulfate proteoglycans, sulfatides, brain α -dystroglycan and $\alpha 3\beta 1$ integrin were found on G4 and G5. The binding site for HNK-1 is located on the G2 subdomain (marked by an arrow in Figure 2).^{26,27}

A 21mer peptide laminin fragment KGVSSRSYVGCICKNLEISRST (**4**) (please see Scheme 1) derived from the second G module (G2 domain) of the $\alpha 1$ -chain was recognized as a binding partner for the HNK-1 oligosaccharide carrying glycolipid.²⁸ Also in the G5 domain one can find the crucial part of the 21mer peptide laminin fragment KGVSSRSYVGCICKNLEISRST (**4**) (blue strand in the right part of Figure 2). The 21mer peptide laminin fragment is used here as a receptor fragment with potential binding specificity for the HNK-1 epitope as well as for the glycomimetic peptides **2** and **3**. The sequence enabled us to find a similar structural motif in another laminin domain for which an X-ray structure exists. Therefore, we replaced the essential amino acid residues in this structural motif by binding-relevant residues of the 21mer peptide **4** in order to construct a reliable HNK-1 binding site model for *in silico* studies of the three ligands: glycomimetic peptides **2** and **3** and the HNK-1 trisaccharide **1**.

Experimental Section

Peptides **2** and **3** were synthesized as reported previously.²³ The 21mer peptide **4** that is a part of the G-domain sequence of the laminin $\alpha 1$ chain was obtained as described.^{27,28} Preparation of the HNK-1 antigen-related trisaccharide **1**, namely propyl (3-*O*-sulfo- β -D-glucopyranosyluronic acid)-(1 \rightarrow 3)-(β -D-galactopyranosyl)-(1 \rightarrow 4)-2-acetamido-2-deoxy- β -D-glucopyranoside (disodium salt) (Figure 1) was performed according to general synthetic schemes developed previously²⁹ and will be published elsewhere.

1D-NMR Experiments. The binding of **1** and **2** to **4** was monitored by ¹H NMR titration experiments. The concentration of **4** (4 mM) in water was kept constant during the experiments. NMR spectra of complexes between **1** and **4** as well as **2** and **4** were recorded at 750 MHz by dissolving 4 mM of **1** or **2** in 0.5 mL of 4 mM solution of compound **4**. The variable temperature unit was calibrated using an external temperature reference sample of ethylene glycol (Bruker).³⁰

2D-NMR Experiments. Samples were prepared by dissolving the lyophilized powder of **2** in 0.5 mL of 20 mM phosphate buffer (90% H₂O, 10% D₂O) at pH 7. ¹H NMR spectra of **2** were recorded on Bruker AMX-700 and AMX-750 MHz spectrometers. The 2D-TOCSY and 2D-NOESY experiments were performed in the phase-sensitive mode using the time proportional phase incrementation (TPPI) method for quadrature detection in the F1 dimension.³¹ A data matrix of 1K \times 512 points was applied to digitize a spectral width of 9000 Hz. Sixty-four scans were taken per increment with a relaxation delay of 1 s. Prior to Fourier transformation, zero filling was applied in the F1 dimension to expand the data to 2K \times 512. Baseline correction was achieved in both dimensions. The corre-

sponding changes in chemical shift of amide signals were optimized for the different spectra. The 2D-TOCSY spectra were acquired with MLEV-17³² during the 60 ms of isotropic mixing period. The 2D-NOESY experiments³³ were carried out with mixing times of 50, 125, 150, and 200 ms. All NMR spectra were recorded at 300 or 310 K.

2D-NOESY and 2D-TOCSY NMR spectra were analyzed using the SPARKY software,³⁴ and all the chemical shift values were referenced to DSS (sodium 4,4-dimethyl-4-silapentane-1-sulfonate). The assignment of the chemical shift values was determined using the standard sequential assignment method of Wüthrich.³⁵

NMR Assignments and Structure Calculation of Compound 2. A 50 ps MD (molecular dynamics) simulation³⁶ with a 2 Å distance between NH of Leu1 and CO of D-Leu6 at 300 K was achieved in order to generate the initial structure of **2**. This step was followed by cyclization and energy minimization using the program INSIGHTII/DISCOVER (Accelrys Inc., San Diego, CA) and the consistent valence force field (cvff). No hydrogen bond restraints were applied for structure calculation. Partial charges were calculated and a distance-dependent dielectric constant was set to $\epsilon = 4r$ in DISCOVER (Accelrys Inc.) on an Octane 2 Silicon Graphics Workstation.

By the application of 27 inter-residue and 18 intra-residue NOE restraints, a 50 ps MD simulation was started at a simulation temperature of 300 K to generate the initial structure, which was further heated up to 900 K in steps of 100 K. The temperature was then reduced to 300 K in steps of 100 K. At each step a MD simulation was carried out again using the NOE constraints. For each stage a cluster of an energy-time graph was produced and the lowest energy structure for a further MD simulation was selected. Eight families of conformers that satisfied the NMR data were obtained. To analyze the convergence, the structures in each family were superimposed on the average structure of each family. An average structure was taken from each family and subjected to low-temperature dynamics at 300 K with NMR constraints. Thereafter, an energy minimization for these structures was carried out. An average structure was taken and an (8 Å)³ box of water molecules was added. Additionally, a MD simulation of 50 ps at 300 K was performed. Twenty conformations with the lowest energy were selected again from a cluster of an energy-time-distance graph. The molecular models thus obtained were energetically minimized using NOE constraints in the presence of H₂O, applying the steepest gradient method. This procedure was repeated with a conjugate gradient for energy minimization.^{37,38} Force constants for bonds and angles were set to 100 kcal (= 418.68 kJ) (mol. Rad²)⁻¹.

Molecular Modeling of the Ligands. The initial 3D structure of **1** was constructed with help of the SWEET-II³⁹ interface of the

- (26) Hall, H.; Deutzmann, R.; Timpl, R.; Vaughan, L.; Schmitz, B.; Schachner, M. *Eur. J. Biochem.* **1997**, *246*, 233.
 (27) Hall, H.; Liu, L.; Schachner, M.; Schmitz, B. *Eur. J. Neurosci.* **1993**, *5*, 34.
 (28) Hall, H.; Vorherr, T.; Schachner, M. *Glycobiology* **1995**, *5*, 435.
 (29) Kornilov, A. V.; Sherman, A. A.; Kononov, L. O.; Shashkov, A. S.; Nifant'ev, N. E. *Carbohydr. Res.* **2000**, *329*, 717.
 (30) Ammann, C.; Meier, P.; Merbach, A. E. *J. Magn. Reson.* **1982**, *46*, 319.
 (31) Marion, D.; Wüthrich, K. *Biochem. Biophys. Res. Commun.* **1983**, *113*, 967.

- (32) Bax, A.; Davis, D. G. *J. Magn. Reson.* **1985**, *65*, 355.
 (33) Kumar, A.; Ernst, R. R.; Wüthrich, K. *Biochem. Biophys. Res. Commun.* **1980**, *95*, 1.
 (34) Goddard, T. D.; Kneller, D. G. *Sparky3*; University of California: San Francisco, 2007.
 (35) Wüthrich, K. *NMR of proteins and nucleic acids*; John Wiley and Sons, Inc.: New York, 1986.
 (36) Sutcliffe, M. J. In *NMR of Macromolecules: A Practical Approach*; Roberts, G. C. K., Ed.; Oxford University Press: New York, 1993; p 359.
 (37) Ajikumar, P. K.; Vivekanandan, S.; Lakshminarayanan, R.; Jois, S. D.; Kini, R. M.; Valiyaveetil, S. *Angew. Chem., Int. Ed.* **2005**, *44*, 5476.
 (38) Liu, J.; Ying, J.; Chow, V. T.; Hruby, V. J.; Satyanarayanan, S. D. *J. Med. Chem.* **2005**, *48*, 6236.
 (39) Bohne, A.; Lang, E.; von der Lieth, C. W. *Bioinformatics* **1999**, *15*, 767.
 (40) Lütteke, T.; Bohne-Lang, A.; Loss, A.; Goetz, T.; Frank, M.; von der Lieth, C. W. *Glycobiology* **2006**, *16*, 71R.

Table 1. Proton Chemical Shift Values (δ , in ppm) for **3** Recorded at 310 K

| residues | H _N | H _{α} | H _{β1} , H _{β2} | H _{γ1} , H _{γ2} | H _{δ} |
|----------|----------------|----------------------------------|---------------------------------------------------------------------|-----------------------------------------------------------------------|----------------------------------|
| L1 | 8.920 | 4.371 | 1.596, 1.661 | — | 0.805, 0.870 |
| S2 | 8.218 | 4.667 | 4.118, 3.943 | — | — |
| E3 | 8.446 | 4.057 | 2.098 | 2.204, 2.479 | — |
| T4 | 7.961 | 4.266 | 4.188 | 1.124 | — |
| T5 | 7.380 | 4.353 | 4.118 | 1.055 | — |
| I6 | 8.523 | 4.161 | 1.563, 1.580 | — | 0.851, 0.896 |

Web site <http://www.glycosciences.de>.^{40,41} The conformational space available to **1** was analyzed by performing a 1 ns-long simulation under vacuum conditions at 400 K. Although both glycosidic linkages populate two major conformations, the trisaccharide exhibits a rather linear, stretched shape overall. A representative conformation from the end of the MD simulation was selected and subsequently used for further considerations. For visualization and overlay of both structures, the INSIGHT-II program was applied. Partial charges for **1**, **2**, and **3** were calculated with the MNDO methods of the MOPAC software package.⁴² The structure of **3** in water was calculated with Gaussian03 (RBLYP/6-31G*)⁴³ on the basis of a NMR structure obtained in DMSO solution.²³

Molecular Docking Experiments. Molecular docking studies between **1**, **2**, or **3** with **4**, or with a model receptor in which the binding-relevant part of **4** has been inserted, were performed with the Arguslab 4.01 software⁴⁴ using gadock and the Hyperchem 8.0 professional software package⁴⁵ with the CHARMM27 force field.

Results and Discussion

In a first step we analyzed the conformations of the cyclic glycomimetic peptide **2** with its negatively charged amino acid residue in the solvent water. The structural data of compound **2** in water enable us to directly compare its shape and the positions of the different functional groups with those of the glycan (**1**).

NMR Structure Calculation of 2. Distance restraints derived from a 2D-NOESY experiment with a mixing time of 150 ms were mainly used for structure calculation of **2**. Peaks involving non-exchangeable protons were scaled to the distance of 1.9–3.0 Å for ($d_{\text{N}\alpha}(i, i)$) and 2.0–3.6 Å for ($d_{\text{N}\alpha}(i, i+1)$). Peaks with exchangeable amide protons ($d_{\text{NN}}(i, i+1)$) were scaled between 2.2 and 4.5 Å interproton distances. For those cross peaks involving methyl and/or methylene groups, a pseudo atom approximation was used.³⁵

The amide region of the 1D-NMR spectrum of the peptide showed good dispersion of chemical shifts over a range of 1 ppm,^{37,46,47} indicating a well-defined conformation of the peptide in aqueous solution. There was no overlap of resonances, except that peaks from minor conformers were observed to have about 20% of the population. The amide region of the NOESY spectrum of the peptide displayed cross peaks between the NH group of Glu3 and the NH group of Thr4, and the NH group of Thr4 and the NH group of Thr5. The NOE contact between the

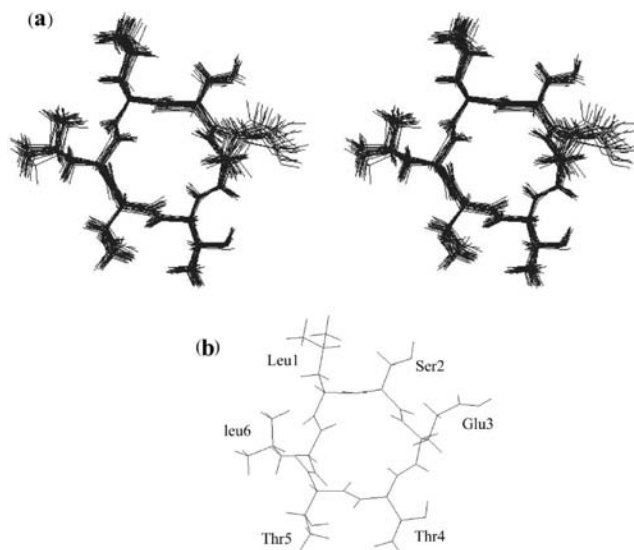


Figure 3. (a) Stereoview representation of 20 best-superimposed NMR structures of **2**, obtained from the NOE-restrained simulated annealing procedure by application of INSIGHT-II. The rms deviation between all superimposed backbone structures was 0.14 Å. (b) Mean ensemble structure of the c-(LSETTI). The program MOLMOL⁴⁸ was used to generate these figures.

NH group of D-Leu6 (hereafter denoted as leu6) and the NH group of L-Leu1 suggests the possibility of folded structure or β -turn structure around these residues.

The NOESY spectra (data not shown) contained both intraresidue ($d_{\text{N}\alpha}(i, i)$) and sequential ($d_{\text{N}\alpha}(i, i+1)$) NOE cross peaks for all the residues from Leu1 to leu6. The NOESY intensities of the cross peaks are shown in the bar graph (see Supporting Information). Furthermore, medium-range NOEs ($d_{\text{N}\alpha}(i, i+2)$) were detectable between Ser2 and Thr4 residues. A distinct NOE cross peak was observed for the leu6H α –Ser2H N distance in the cyclic peptide. Two set of peaks have been observed for this peptide in the 1D ¹H NMR spectrum. There were major populated (more than 80% in intensity) peaks and minor (less than 20%) populated peaks (Supporting Information). This phenomenon is very common in the case of peptides. So, it is possible that the peptide is interconverting between major and minor conformation in μs to ms time scale of motion. However, the represented structure is calculated from the major conformation (cross peaks that showed up more than 80% population).

The ¹H α chemical shift (Table 1) deviations from the random coil values were calculated for all the residues (see Supporting Information) of cyclic peptide c-(LSETTI). Interestingly, S2 shows a positive chemical shift deviation whereas negative proton chemical shift deviations were observed for the residues of E3, T4 and I6 (Supporting Information Figure 3S). Taken together, these results indicate that the peptide adopts a folded conformation in solution. A total of 45 distance constraints were observed that clearly define the conformation of the peptide in solution. Twenty superimposed structures that satisfy the NMR data based on NMR-restrained MD simulations are shown in Figure 3a. The average rms deviations of the backbone atoms were 0.14 Å, indicating the convergence nature of the energy-minimized structure (Figure 3b). The backbone structure of the peptide is characterized by a weak β -turn consisting of Ser2, Glu3, Thr4 and Thr5. The existence of a β -turn structure is supported by NOEs between H N –H N ($i, i+1$) of these residues and H α of Ser2 to Thr4 H N ($i, i+2$) NOEs, and also the dihedral

(41) von der Lieth, C. W. In *Comprehensive Glycoscience*; Kamerling, J. P., Ed.; Elsevier: Oxford, 2007; Vol. 2, p 329.

(42) Stewart, J. MOPAC 7, 2007.

(43) Frisch, M. J. et al.; *Gaussian 03, Revision B.03*; Gaussian, Inc.: Pittsburgh, PA, 2003.

(44) Thompson, M. A. *Arguslab 4.0.1*; Planaria Software LLC: Seattle, WA, 2004.

(45) *Hyperchem 8 prof.*; Hypercube: Gainesville, FL, 2007.

(46) Jining, L.; Makagiansar, I.; Yusuf-Makagiansar, H.; Chow, V. T.; Siahann, T. J.; Jois, S. D. *Eur. J. Biochem.* **2004**, *271*, 2873.

(47) Wishart, D. S.; Bigam, C. G.; Holm, A.; Hodges, R. S.; Sykes, B. D. *J. Biomol. NMR* **1995**, *5*, 67.

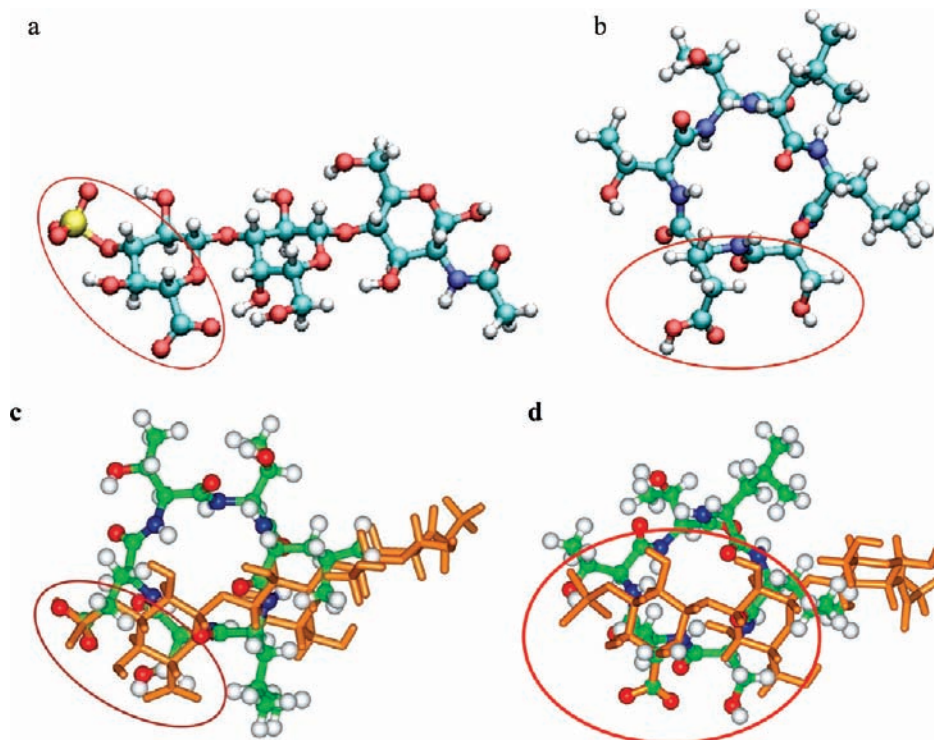


Figure 4. Comparison between the shapes of compounds **1** and **2**. (a) Model structures of trisaccharide **1** in ball and stick presentation. (b) Model structure of cyclopeptide **2** in ball and stick presentation. Overlay-structures of trisaccharide **1** (stick presentation in orange) and **2** (ball-and-stick presentation), (c) aligning the sulfate group of **1** and the carboxyl group of **2** or (d) aligning the carboxyl groups. The regions where the cyclic peptide mimics the trisaccharide are highlighted.

angle of these residues indicates the existence of a β -turn structure that is nearly type I. The structure of the cyclic peptide c-(LSETTI) was calculated based on NOEs and no hydrogen bond constraints were used for structure calculation. However, we observed hydrogen bonds between the hydroxyl group of Thr5 and the carbonyl group of Thr4, between Thr4-CO and leu6-H^N, and between Thr5-CO and Leu1-H^N as well as between Leu1-CO and Glu3-H^N of the corresponding amino acid residues in all the calculated conformations.

Structural Comparison of Compounds 1 and 2. Once the NMR structure of **2** was solved (including the analysis of its conformational dynamics), we compared the model structures of **1** and **2** with each other (Figure 4). At first glance both molecules seem to have little structural similarities (Figure 4a–d). However, taking into account their physicochemical properties, it becomes apparent that both molecules exhibit a negatively charged site and a neutral, more hydrophobic site. Especially the charged groups present in **1** and **2** suggest that various modes of overlay for both structures will lead to further insights. In contrast to **2**, compound **1** has two negatively charged functional groups: the carboxyl group of the glucuronic acid and the sulfate group at the C3 atom of the same carbohydrate moiety. The MD simulation revealed that the distance between both groups (around 6 Å) is rather stable. Both negatively charged groups of **1** were overlaid with the carboxyl group of glutamic acid of **2** (Figure 4c, d). For both modes of superposition, the hydrophobic face of either the galactose or the *N*-acetylglucosamine ring could be spatially aligned with a hydrophobic side chain of one of the two adjacent leucine residues.

These findings suggest that the combination of a negative charge and hydrophobic patches within a clearly defined distance contribute to the specificity of recognition for both molecules (**1** and **2**) by a particular HNK-1 receptor. In comparison to the two glycomimetic peptides under study (**2** and **3**) the conformational flexibility of **1** is much higher due to its oligosaccharide character. However, one has to consider that the 3-*O*-sulfo-GlcA-residue of **1** is the essential contact region. The second cyclic glycomimetic peptide (**3**), however, does not have a negatively charged group. Therefore, a detailed conformational comparison of **2** and **3** was performed in different solvents to study the structural similarities and dissimilarities between these two cyclic peptides.

Conformational Comparison between Compounds 2 and 3 in Water and in DMSO. Compound **2** mainly populates as a single conformer cluster in aqueous solution (Figure 3). The model structures derived from NOE data of **2** in water have fewer hydrogen bonds than the NMR structures of **2** in DMSO (Figure 5). However, these hydrogen bonds should clearly be identified and considered when discussing deviations between water- and DMSO-derived NMR structures. This statement is strongly supported by results from NMR experiments of oligosaccharides carried out in water, DMSO or DMSO/water solutions.^{49–52} With the help of the NMR data obtained for **2** analyzed in water and in DMSO it was possible to calculate

(48) Koradi, R.; Billeter, M.; Wüthrich, K. *J. Mol. Graph* **1996**, *14*, 51.

(49) Siebert, H. C.; André, S.; Asensio, J. L.; Cañada, F. J.; Dong, X.; Espinosa, J. F.; Frank, M.; Gilleron, M.; Kaltner, H.; Kozár, T.; Bovin, N. V.; von der Lieth, C. W.; Vliegthart, J. F. G.; Jiménez-Barbero, J.; Gabius, H. J. *ChemBiochem* **2000**, *1*, 181.
 (50) Siebert, H. C.; André, S.; Vliegthart, J. F. G.; Gabius, H. J.; Minch, M. J. *J. Biomol. NMR* **2003**, *25*, 197.

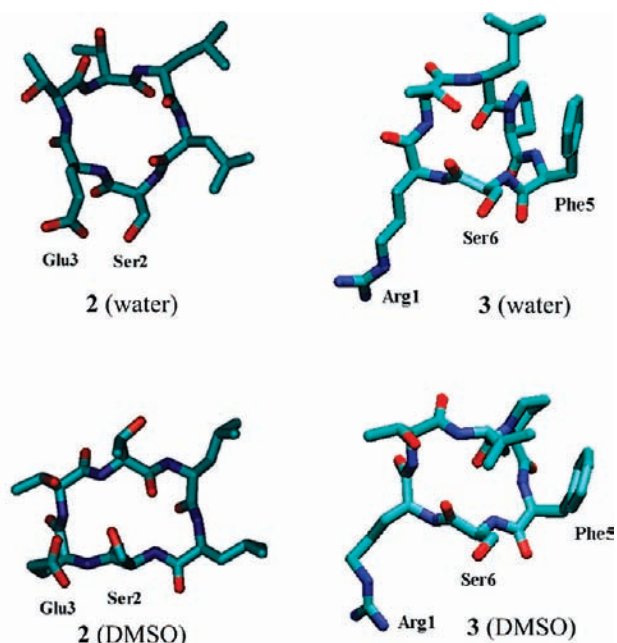


Figure 5. Comparison of minimum energy conformations of cyclic peptides **2** and **3** in water and DMSO solutions. The main amino acid residues that are responsible for a specific binding with a HNK-1 receptor are labeled.

the conformation of **3** in a water environment from its conformation in DMSO²³ in a reliable way (Figure 5).

The structural models of **2** and **3** in water provide valuable insights into the binding mechanisms of these glycomimetic peptides with receptors of HNK-1. No significant differences exist between the DMSO and water structure of **3**; thus, the nearly identical conformations are not dependent on the solvent and clustering method.⁵³

Our comparison of structure and dynamics of compounds **2** and **3** indicates that the pronounced, positive Arg residue of **3** could play a role that is similar to that of the negatively charged Glu residue of **2** (Figure 5). Thus, it was of interest to test whether negatively charged residues are present in the binding pockets of receptors that interact primarily with negatively charged ligands such as uronic acids and sulfated carbohydrates.

To gain deeper insight on the atomic level as to how glucuronic acids as well as sulfated carbohydrates interact with proteins, we performed a comprehensive analysis of the corresponding protein–glycan complexes deposited in the PDB. The GlyVicinity tool (<http://www.glycosciences.de/tools/glyvicinity/>) was used for this purpose.⁵⁴ Unfortunately, no sulfated derivatives of glucuronic acid were reported in the PDB. Therefore, the interactions of uronic acid (to which glucuronic acid belongs) and those of the sulfated carbohydrate residues were analyzed separately.

Statistical Analysis of Uronic Acid–Protein and Sulfated Carbohydrate–Protein Interactions. The analysis of the non-covalent interaction of uronic acids with specific amino acid

Table 2. Analysis of the Interaction Pattern of Uronic Acid and Sulfated Monosaccharide Residues in Protein–Carbohydrate Complexes Obtained from the Protein Data Bank (PDB)

| aminoacid residue | uronic acid ^a | | sulfated monosaccharide ^b | |
|-------------------|--------------------------|--------------|--------------------------------------|--------------|
| | counts | deviation, % | counts | deviation, % |
| Asp | 74 | 23 | 5 | −91 |
| Glu | 56 | −23 | 26 | −60 |
| Lys | 79 | 16 | 276 | 357 |
| Asn | 101 | 88 | 108 | 126 |
| Arg | 182 | 200 | 212 | 293 |
| Gln | 68 | 44 | 35 | −17 |
| His | 40 | 52 | 49 | 109 |
| Gly | 12 | −85 | 47 | −35 |
| Ser | 38 | −56 | 33 | −57 |
| Ala | 47 | −46 | 44 | −43 |
| Pro | 42 | −28 | 17 | −67 |
| Thr | 73 | 6 | 31 | −50 |
| Ile | 13 | −81 | 9 | −85 |
| Tyr | 88 | 132 | 53 | 57 |
| Val | 21 | −72 | 24 | −64 |
| Cys | 31 | 50 | 3 | −84 |
| Met | 12 | −56 | 4 | −83 |
| Trp | 82 | 423 | 37 | 165 |
| Phe | 55 | 15 | 17 | −60 |
| Leu | 13 | −47 | 11 | −87 |

^a One-hundred eighty-seven uronic acid residues were found in 55 PDB entries. These residues interact with 1171 amino acid units within the spatial vicinity of 4 Å. The deviation in percent from its natural occurrence is given for each amino acid. ^b Two-hundred twenty-one sulfated saccharide residues were found in 54 PDB entries. These residues interact with 1041 amino acids within the spatial vicinity of 4 Å. The deviation in percent from its natural occurrence is given for each amino acid.

residues reveals a clear preference for residues with positively charged side chains of arginine and lysine as well as with histidine and the neutral amino acid asparagine (Table 2). Viewed from the uronic acid residues, the carboxyl group is clearly the dominating (about 25% of all contacts with proteins) and strongest (average distance 3.0 Å) interaction partner, which indicates that this group exhibits essentially ionic interactions or strong hydrogen bonds. The most prominently interacting atoms are the nitrogen atoms of the side chains of arginine, asparagine and lysine.

For the tyrosine residues occurring in the vicinity of uronic acids the terminal OH group of tyrosine (about 50% of all contacts) is the dominant interaction partner, stabilizing binding via hydrogen bonds. The negatively charged Asp as well as all hydrophilic amino acid residues are markedly overrepresented in the vicinity of uronic acid.

Sulfate residues strongly interact with positively charged atoms of the side chains of Lys, Arg, and His (Table 2). As expected, residues with negative charges are clearly underrepresented (Glu: 60%, Asp: 91%). However, they can be present, as displayed in Table 2. In the case of the laminin fragment **4**, the Glu residue at position 16 underlines this finding. Interactions with lysine exhibit by far the most frequent and strongest contacts. They can be regarded as highly characteristic for this type of interaction. The terminal nitrogen atoms of the guanidino group from the Arg side chain are also strong and frequent interaction partners of sulfated carbohydrates (Table 2). Residues Lys and Arg account for about half of all detected interactions with sulfated residues. The only other frequent contacts are formed with the carboxamide group of Asn and the two nitrogen atoms of the imidazole ring of the His side chain.

On the basis of data from the PDB, the positively charged Arg and Lys residues (also present in compound **4**) have a much

(51) Siebert, H. C.; Frank, M.; von der Lieth, C. W.; Jiménez-Barbero, J.; Gabius, H. J. In *NMR of Glycoconjugates*; Jiménez-Barbero, J., Peters, T., Eds.; Wiley-VCH: Weinheim, 2003; p 39.

(52) Siebert, H. C.; Jiménez-Barbero, J.; André, S.; Kaltner, H.; Gabius, H. J. *Methods Enzymol.* **2003**, *362*, 417.

(53) Guthöhrlein, E. W.; Malesevič, M.; Majer, Z.; Sewald, N. *Biopolymers* **2007**, *88*, 829.

(54) Lütke, T.; Frank, M.; von der Lieth, C. W. *Nucleic Acids Res.* **2005**, *33*, D242.

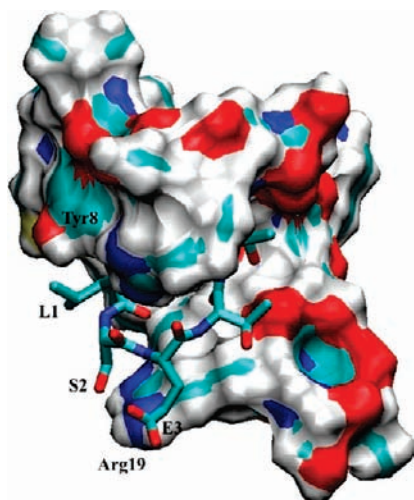


Figure 6. Snapshot from a MD simulation of **2** in a stable binding mode with **4**.

higher percentage in comparison to their natural occurrence in proteins when analyzing their interactions with sulfated pyranosides (Table 2). In the case of Lys, the observed deviation is much higher than 100%. As indicated by the statistical analysis (Table 2), it is very likely that Lys13 contributes to complex formation. This assumption is strongly supported by NMR analysis and MD simulations of compound **4** interacting with **1** and **2** (see next paragraph).

NMR Titration Studies and Molecular Modeling with Compound 4. The major question concerning the binding behavior of **1** and **2** with respect to **4** can be addressed with the help of NMR titration methods. Indeed, chemical shift alterations of the Asn14 (which is next to Lys13) and Arg19 proton NMR signals are detectable when **1** or **2** is added to **4** (Supporting Information). A NMR signal of the Tyr8 residue of **4** shows an upfield shift of 0.02 ppm after a complex with **1** has been formed. The fact that the signal alterations of residues Asn14 and Arg19 of **4** are not significantly upfield shifted when a complex with **2** has formed points to a weaker binding between **2** and **4** (comparing with the shift alterations after **3** was added to **2**). The results of this NMR titration study enabled us to suggest energy-minimized models of complexes between **2** and **4**. The negatively charged carboxyl group of Glu3 of compound **2** (Figure 5) interferes with the Arg19 and Lys13 residues of **4**. Furthermore, hydrophobic interaction exists between Tyr8 of **4** and the two Thr residues of **2** (Figure 6).

It has already been shown that linear peptides can give valuable information concerning the involvement of certain amino acid residues when studying carbohydrate–peptide interactions.^{55,56} It has also been demonstrated that specific interactions between 15mer peptides and the Thomsen-Friedenreich antigen (TF, Gal β -(1 \rightarrow 3)GalNAc α) can successfully be analyzed with a strategic combination of NMR techniques and molecular modeling tools.⁵⁵ In the same way it was possible to examine the interactions between 15mer peptides and the pentasaccharide chain of ganglioside GM₁.⁵⁶ By analyzing the

TF antigen in complex with each of the three TF-specific 15mer peptides via NMR and molecular modeling methods, we have found that in two of the three peptides Arg residues are involved in binding interactions with the disaccharide. For the third peptide, the side chain of a Ser residue and aromatic amino acid residues were identified as relevant for binding.⁵⁵ With the same combination of methods it was possible to show which amino acid residues stabilize complexes between three different GM₁-specific 15mer peptides and the pentasaccharide chain of ganglioside GM₁.⁵⁶ For two peptides, Arg residues and aromatic amino acids are responsible for an interaction with the negatively charged pentasaccharide chain. In the case of the third GM₁-specific 15mer peptide, a Lys residue and aromatic amino acids are important for the formation of a stable oligosaccharide-peptide complex. It is of note that we were also able to identify these amino acids (Arg, Lys and Tyr) in the 21mer laminin fragment (compound **4**) as being the crucial contact points for **1** and **2**. However, the drawback of interaction studies with linear peptides is their flexibility. NMR spectra of **4** in its free and ligand-bound state clearly show that multiple conformations are present in solution. The structural model shown in Figure 6 represents a minimum energy conformation and is in full agreement with the NMR results. Figures of compound **4** in complex with **1** and **3** are shown in the Supporting Information section. Since the MD simulations indicate that various other possibilities of complex formation are energetically allowed, an improved receptor model beside compound **4** was generated.

Molecular Modeling of 1, 2, and 3 Interacting with an Improved Receptor Model That Contains the Binding-Relevant Part of Compound 4. To work with an improved receptor model we incorporated the binding-relevant part of compound **4** into a proper template structure. Although this template structure represents the murine laminin α -1LG5 domain and not the α -1LG2 domain in which the HNK-1 binding site is found, the overall structure of all laminin G domains is similar.^{57–60} The sequence homology of **4** with a part of the murine laminin α -1LG5 domain was found by a Blast search (see Supporting Information and Figure 7). For a sequential comparison between the murine and human laminin α -1LG2 domain, please see also Supporting Information.

To scrutinize the binding specificity of **1** and **2** with a receptor structure of higher rigidity we constructed a model structure for our final molecular docking calculations. With the designed HNK-1 receptor structure it is now possible to analyze the second HNK-1 receptor-specific cyclic glycomimetic peptide, that is compound **3**,²³ in detail. In the final docking study we analyzed the binding affinities of **1**, **2**, and **3** for the constructed HNK-1 model receptor. This model receptor is based on the laminin α -1LG5 structure in which 15 amino acid residues SYVGCINKLEISRST of **4** (Figure 7) have been inserted after the corresponding part in the α -1LG5 domain had been removed.

The model receptor enabled us to analyze potential contact points in the context of well-defined binding site architecture (as compared to the rather flexible compound **4**). We started

(55) Siebert, H.-C.; Lu, S. Y.; Frank, M.; Kramer, J.; Wechselberger, R.; Joosten, J.; André, S.; Rittenhouse-Olson, K.; Roy, R.; von der Lieth, C. W.; Kaptein, R.; Vliegenthart, J. F. G.; Heck, A. J.; Gabius, H. J. *Biochemistry* **2002**, *41*, 9707.

(56) Siebert, H.-C.; Born, K.; André, S.; Frank, M.; Kaltner, H.; von der Lieth, C.-W.; Heck, A. J. R.; Jiménez-Barbero, J.; Gabius, H.-J. *Chem.—Eur. J.* **2006**, *12*, 388.

(57) Harrison, D.; Hussain, S. A.; Combs, A. C.; Ervasti, J. M.; Yurchenco, P. D.; Hohenester, E. *J. Biol. Chem.* **2007**, *282*, 11573.

(58) Tisi, D.; Talts, J. F.; Timpl, R.; Hohenester, E. *Embo J.* **2000**, *19*, 1432.

(59) Wizemann, H.; Garbe, J. H.; Friedrich, M. V.; Timpl, R.; Sasaki, T.; Hohenester, E. *J. Mol. Biol.* **2003**, *332*, 635.

(60) Carafoli, F.; Clout, N. J.; Hohenester, E. *J. Biol. Chem.* **2009**, *284*, 22786.

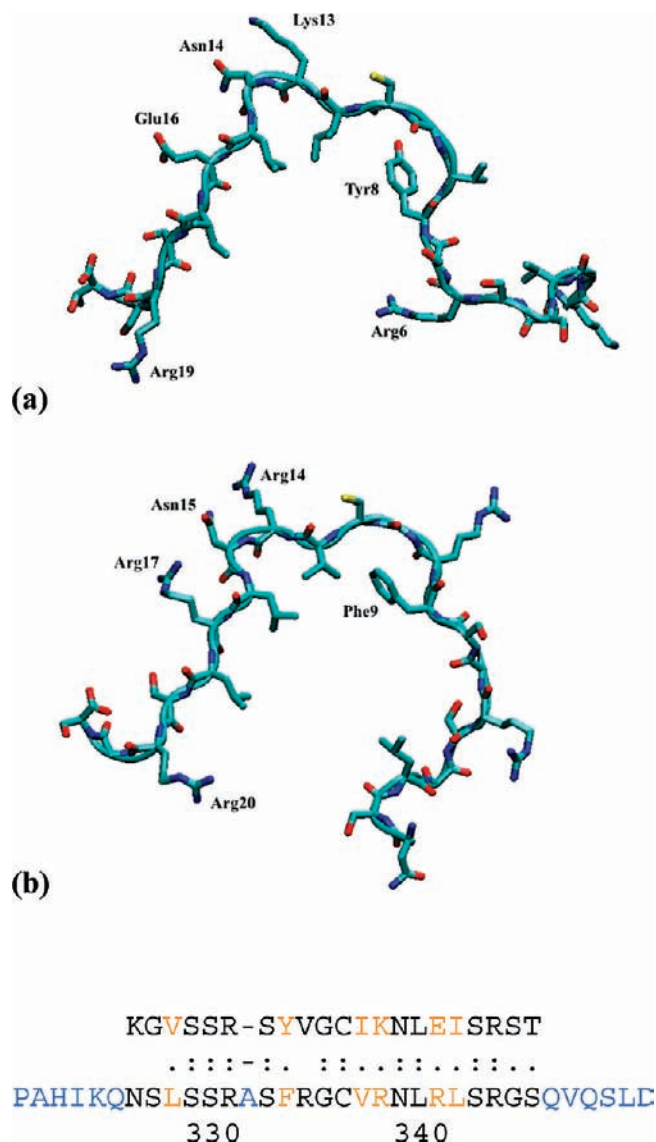


Figure 7. (a) Structural alignments of **4** as a component of the laminin α -ILG2 domain with (b) its corresponding part in the murine laminin α -ILG5 domain. To perform this alignment the dihedral angles of the homologous part in the murine laminin α -ILG5 domain (b) were transferred to the 21 amino acid residues of the laminin α -G2 domain which match compound **4** (a).

our final docking analysis with **1** and found that the two negatively charged groups of the sulfated glucuronic acid are the most important functional groups for the formation of a stable contact with Lys13 (Figure 8a).

Different docking positions of **1**, **2**, and **3** were tested in accordance to the NMR and modeling derived results described above. In summary, the negative charge of Glu3 of **2** corresponds to the negative charges of the carboxyl or sulfate groups of 3-sulfated glucuronic acid of compound **1** (Figure 8b). It appears, however, that not only the negative charge is responsible for the recognition of both molecules (**1** and **2**); a neutral, more hydrophobic site of **1** or **2** contributes to a stable complex as well. This means that similarities in shape and distance of crucial functional groups (carboxyl group, hydroxyl groups) and the hydrophobic/hydrophilic character of **1** and **2** (Figure 4a,b) are essential structural determinants for their binding specificity for laminin and other HNK-1 binding receptors. The model

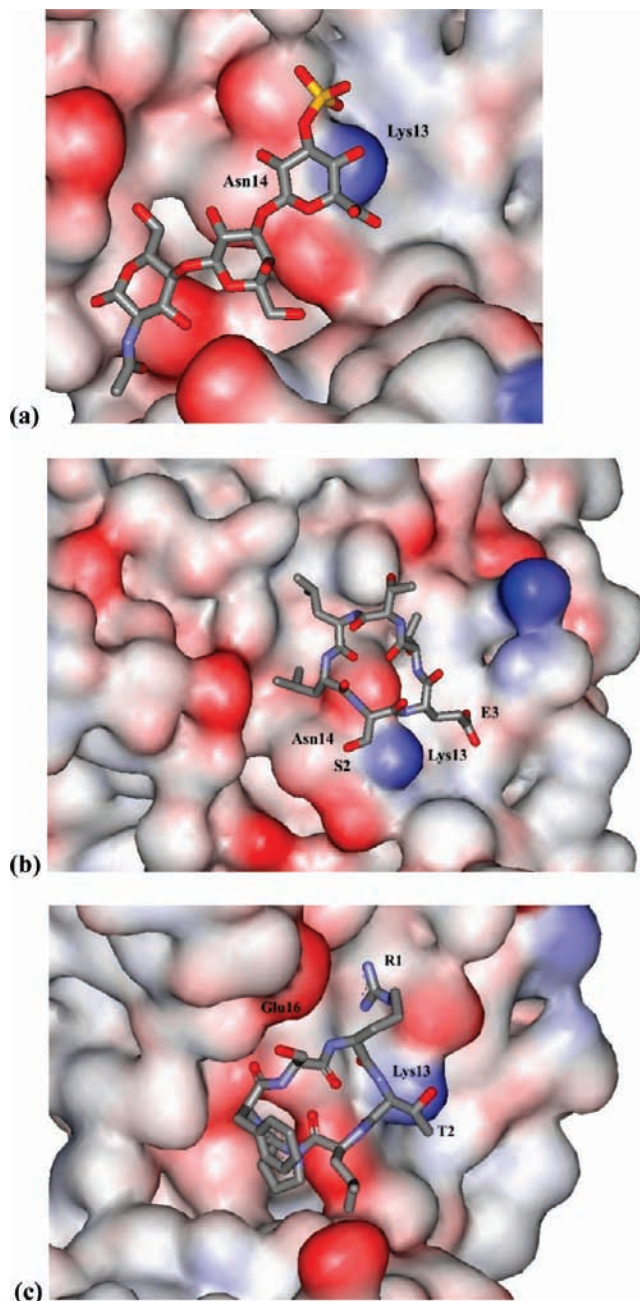


Figure 8. Compounds (a) **1**, (b) **2** and (c) **3** are shown in complex with the receptor structure in which the binding-relevant peptide sequence SYVGCIKNLEISRST of **4** (the laminin α -ILG2 domain) has been inserted into the laminin G4/G5 domain.

ligand structures presented in Figure 8a–c are the energetically most favorable ones as revealed by our docking studies.

In contrast to the NMR and molecular modeling-based structural comparison of **1** vs **2**, it is not so easy to understand why **3**, with its positively charged Arg residue, also mimics **1**. Nevertheless, as shown in Table 2, in addition to positively charged and hydrophobic contact points, Glu residues are also found in the binding sites of receptors of uronic acids and (to a lesser extent) of sulfated carbohydrates. Compound **4** indeed contains a Glu residue (Glu16; see Figure 6). Therefore, the hydrophobic Phe residue and the positively charged Arg residue of **3** are in principle also able to form proper and stable complexes with the laminin-derived receptor structure (Figure 8c).

When the crucial amino acid residues SYVGCINKLEISRST from **4** (the 21mer fragment of the laminin G2 domain) are inserted into the laminin α -1LG5 domain (from the amino acid position 3014 to 3029 in the B-chain), only a rather shallow binding pocket is formed. The polarities and charges of the crucial amino acids at the HNK-1 binding site are essential for the binding affinities of **1**, **2**, and **3**.

The interactions of compound **1** with the HNK-1 binding site of the laminin domain model establish a stable complex formation. The two negatively charged functional groups of 3'-sulfated glucuronic acid are in close contact with the positively charged Lys residue (at position 3026) of the HNK-1 binding site. These two functional groups (sulfate and carboxylic group) enclose the Lys residue. Furthermore, the C4 OH group between the charged residues of 3'-sulfated glucuronic acid establishes a hydrogen bond to the Lys residue. The HNK-1 receptor binding is additionally supported by a hydrogen bond contact of the oxygen at the *N*-acetyl C atom of GlcNAc to Ser (at position 3038).

When comparing the negative binding energies of **2** and of **1** in complex with our model receptor we learn that the glycomimetic peptide **2** binds in a less favorable way (54.8 kJ/mol weaker) than the glycan (**1**). In this regard, we have to consider that in contrast to **1** compound **2** has only one negatively charged group. Furthermore, fewer and weaker hydrogen bonds are established by **2** when interacting with the HNK-1 binding site in the modeled laminin domain. For example, a Thr residue of **2** forms via its NH hydrogen atom a stable hydrogen bond with the carboxylic CO group of Glu (at position 2904). The same nitrogen atom (acting as acceptor) is involved in a hydrogen bond to a water molecule. In the Supporting Information section the reader can find this text-part in which all acceptors and donors are indicated in brackets by (A) and (D).

Furthermore, our calculations with the modeled laminin domain clearly show that no deep characteristic binding pocket for HNK-1 or its glycomimetic peptides exists and that the ionic interactions and polarities are dominating the interaction process. Therefore, the conformation of the ligand (HNK-1 trisaccharide) seems to be less important when interacting with the HNK-1 binding site of laminin.

One can estimate the conformational entropy of HNK-1 from the population of the potential energy map or from the fraction of populated surfaces in the MD simulations. The HNK-1 trisaccharide consists of β 1-3 and β 1-4 glycosidic linkages. This trisaccharide itself is linear. No correlations exist between both linkages and they can be considered as independent. The conformational entropy for lactose and for *N,N'*-diacetyl chitobiose, which is very similar to the case discussed here, has been described in the literature.⁶¹⁻⁶³ The conformational entropy at 300 K amounted to ca. 8.5-9 kJ/(mol K). Therefore, the complete freezing of this ligand upon binding would represent an entropy loss of about 17-18 kJ/(mol K) and freezing of one of the linkages, half of it.

The second glycomimetic peptide **3**, however, which has no negatively charged group at all but a positively charged Arg residue, is the best binding partner for the modeled laminin domain. The affinity of **3** is even better (25.5 kJ/mol) than that of **1**. In looking at the HNK-1 binding site in detail, we recognize that the vicinity of the Lys residue is negatively polarized and that the Arg residue of **3**, with its long flexible side chain, can fit perfectly to this negatively polarized region of the HNK-1 model receptor. Due to such a fit, the formation of more stabilizing hydrogen bonds is induced. The N atom of the Ser residue of **3** thus establishes a hydrogen bond to the Ser OH (at position 3038) residue of the laminin domain. Furthermore, a hydrogen bond exists between the NH group of the Arg residue of **3** and the CO group of Lys (at position 3026). Two additional hydrogen bonds are present between Pro and Thr residues of **3** and two water molecules. As shown in Figure 8S (Supporting Information) the Arg residue is indeed of great importance since a lack of the Arg-Glu contact between the cyclic peptide and the laminin fragment as well as an replacement of Arg by Ala in compound **3** lowers the binding energy significantly.

The comparison between **1**, **2**, and **3** interacting with the modeled laminin domain that contains the binding-relevant part of **4** provides clear hints as to whether and how the two cyclic glycomimetic peptides can be improved within the context of rational drug design. Taking all results of this study together allows us to predict glycomimetic peptides similar to **2** with a potentially higher affinity for HNK-1 receptors. According to our structural studies the replacement of the Ser2 OH group in **2** by a negatively charged group or the replacement of Ser2 by an Asp or Glu residue should increase the binding affinity for HNK-1 receptors. In the case of **3** such modifications are expected to have only a minor impact on the binding affinity. Therefore, our results contribute a new information on whether and how analogous cyclic glycomimetic peptides of the HNK-1 epitope (**1**) with a potentially improved affinity for HNK-1 receptors can be designed. In addition, cell biological experiments will help to evaluate the effects of such compounds on the growth of motor neurons; the structural aspects of their binding behavior should again be analyzed by a strategic combination of biophysical methods such as surface plasmon resonance, NMR and molecular modeling.⁶⁴⁻⁶⁸

Acknowledgment. The 700 and 750 MHz spectra were recorded at the SON NMR Large Scale Facility in Utrecht, which is funded by the European Union project "EU-NMR-European Network of Research Infrastructures for Providing Access & Technological Advancement in Bio-NMR" (FP-2005-RII3-Contract-no. 026145). The work is also supported by the German Research Foundation

- (61) Asensio, J. L.; Cañada, F. J.; Bruix, M.; Rodriguez-Romero, A.; Jiménez-Barbero, J. *Eur. J. Biochem.* **1995**, *230*, 621.
 (62) Siebert, H. C.; von der Lieth, C. W.; Kaptein, R.; Beintema, J. J.; Dijkstra, K.; van Nuland, N.; Soedjanaatmadja, U. M.; Rice, A.; Vliegthart, J. F.; Wright, C. S.; Gabius, H. J. *Proteins* **1997**, *28*, 268.
 (63) Asensio, J. L.; Siebert, H. C.; von der Lieth, C. W.; Laynez, J.; Bruix, M.; Soedjanaatmadja, U. M.; Beintema, J. J.; Cañada, F. J.; Gabius, H. J.; Jiménez-Barbero, J. *Proteins* **2000**, *40*, 218.

- (64) Siebert, H. C.; André, S.; Lu, S. Y.; Frank, M.; Kaltner, H.; van Kuik, J. A.; Korchagina, E. Y.; Bovin, N.; Tajkhorshid, E.; Kaptein, R.; Vliegthart, J. F. G.; von der Lieth, C. W.; Jiménez-Barbero, J.; Kopitz, J.; Gabius, H. J. *Biochemistry* **2003**, *42*, 14762.
 (65) Siebert, H. C.; Tajkhorshid, E.; Vliegthart, J. F. G.; von der Lieth, C. W.; André, S.; Gabius, H. J. In *NMR spectroscopy and computer modeling of carbohydrates*; ACS Symposia Series; Vliegthart, J. F. G., Woods, R. J., Eds.; American Chemical Society: Washington, D.C., 2006; Vol. 930, p 81.
 (66) Nair, S. S.; Romanuka, J.; Billeter, M.; Skjeldal, L.; Emmett, M. R.; Nilsson, C. L.; Marshall, A. G. *Biochim. Biophys. Acta* **2006**, *1764*, 1568.
 (67) Wu, A. M.; Singh, T.; Liu, J. H.; Krzeminski, M.; Russwurm, R.; Siebert, H. C.; Bonvin, A. M.; André, S.; Gabius, H. J. *Glycobiology* **2007**, *17*, 165.
 (68) Haseley, S. R.; Vermeer, H. J.; Kamerling, J. P.; Vliegthart, J. F. *Proc. Natl. Acad. Sci. U.S.A.* **2001**, *98*, 9419.

(grant SFB 470). This paper is dedicated to the memory of Dr. Claus-Wilhelm von der Lieth and Professor Janusz Dabrowski.

Supporting Information Available: Essential parts of 1D-NMR spectra of **4** before and after the addition of **1** or **2**. Low field region of a one-dimensional ^1H NMR spectrum, summary of NOEs and the proton chemical shift deviations for compound **2**. Sequence alignment of **4** with pdb-structures and blast-based

alignment. The three-dimensional structure of the G1, G2, and G3 domain of $\alpha 2$ laminin. Computational calculation of **1** and also of **3** in a stable binding mode with **4**, a text-part in which acceptors and donors are indicated as well as the complete author list of ref 43. This material is available free of charge via the Internet at <http://pubs.acs.org>.

JA904334S